Limestone powder and silica fume performance on slag-blended PLC plain and self-consolidating mortars properties

Tarek Chiker, Salima Aggoun

Limestone Powder and Silica Fume Performance on Slag-Blended PLC plain and Self-Consolidating Mortars Properties

Tarek Chiker[1], ✉, **Salima Aggoun**[2]

Abstract

Mineral admixtures and waste by-products in concrete exhibit economical and environmental benefits, but their cementing and engineering properties should be assessed before practical adoption. In this study, we investigated hydration and physical properties of Self-Consolidating (SCM) and Ordinary (OM) mortars, based on slag-blended Portland limestone cement (PLC), with equivalent water-to-cement ratio (E/C≈ 0.55). The variables were mortar type and mineral admixture type, limestone powder (LP) or silica fume (SF). Therefore, we made two ordinary mortars (OMs): Oref (OPC-based) and Oplc (slag PLC-based); two self-consolidating mortars (SCMs): SplcL (limestone-based) and SplcS (silica fume-based). We assessed compressive strength, sorptivity, hydration heat, thermogravimetric analysis and SEM images. Results reveal that SCM exhibits similar to better performance than reference mix. Blended LP performs better in SCMs, and seems to have packing role and doesn't contribute to carboaluminate formation. SF is efficient when substituted more than 10%.

Keywords: hydration, limestone powder, microstructure, PLC, silica fume, slag, thermal analysis

Acknowledgments

The authors are very thankful to the L2MGC laboratory staff at CY Paris Cergy Université and LGCE members of Jijel University in Algeria.

[1], ✉ Tarek CHIKER, Ass. Prof., Dr.
Tarek.chiker@cyu.fr or chiker_tarek@yahoo.fr ; https://orcid.org/0000-0003-0236-0619
L2MGC, CY Paris Cergy Université, F9500 Cergy-Pontoise, France
Laboratory of Civil Engineering and Environment, Jijel University, Algeria

[2] Salima AGGOUN, Prof.
Salima.aggoun@cyu.fr ; https://orcid.org/0000-0002-2757-1263
L2MGC, CY Paris Cergy Université, F9500 Cergy-Pontoise, France

Limestone Powder and Silica Fume Performance on Slag-Blended PLC plain and Self-Consolidating Mortars Properties

Abstract

Mineral admixtures and waste by-products in concrete exhibit economical and environmental benefits, but their cementing and engineering properties should be assessed before practical adoption. In this study, we investigated hydration and physical properties of Self-Consolidating (SCM) and Ordinary (OM) mortars, based on slag-blended Portland limestone cement (PLC), with equivalent water-to-cement ratio (E/C≈ 0.55). The variables were mortar type and mineral admixture type, limestone powder (LP) or silica fume (SF). Therefore, we made two ordinary mortars (OMs): Oref (OPC-based) and Oplc (slag PLC-based); two self-consolidating mortars (SCMs): SplcL (limestone-based) and SplcS (silica fume-based). We assessed compressive strength, sorptivity, hydration heat, thermogravimetric analysis and SEM images. Results reveal that Oplc exhibits similar to better performance than Oref; blended LP leads to 36 % higher mechanical strength and more 50 % carboaluminatein SCMs, 40% lower heat and rate of hydration, and seems to have packing role and doesn't contribute to more sites' nucleation, SF is efficient when substituted more than 10%.

Keywords: hydration, limestone powder, microstructure, PLC, silica fume, slag, thermal analysis

1 Introduction

At present day, blended cements and mineral admixtures are worldwide used to meet sustainable development requirements [1,2], and cutting CO_2 emissions. Due to its abundance and economical benefit, limestone powder (LP) gains more confidence in cement [3] and concrete industries. According to PCA [4], PLC reduces project carbon footprint by 10% (see greenercement.com). It is a good option for green circular economy [5].

First, carbonate addition features in cementing network are well known today. That is, it enhances cement hydration by creating favorable nucleation sites allowing the growth of Portlandite hydrate[6], silicate hydrate (S-C-H)[7] and carboaluminate formation ($C_3A.CaCO_3.11H_2O$) [8] or hemicarboaluminate ($C_3A.1/2CaCO_3.1/2Ca(OH_2)$) [9] instead of sulfoaluminate phase [10]. Furthermore, many workers support the fact of accelerating effect of limestone on Portland cement hydration [11] by shortening the dormant period and pronouncing the second peak time [12]. Others state a good packing density within LP mixes[13,14]. Consequently, high mechanical properties at early ages [15,16] as resulted from hydration of tricalcium silicate hydrate (C_3S) has been previously recorded [17]. According to Zhao and Zhang [18], many hydration issues of limestone cement still needing more investigations.

Furthermore, PLC including inter-ground limestone may exhibit similar to better mechanical and durability properties than ordinary Portland cement (OPC) [14,19], especially when finely ground [20,21].

PLC cement limestone substitution is reported in the range of 10 and 25 % [3,22]. However, it has been found that blended PLC may exhibit higher performances [23,24], especially in the presence of aluminosilicate or pozzolanic sources (slag, pozzolana…) [25], due to performed hydrate dilution , leading to increased LP substitution rate [26]. Actually, alumin allows additional replacement by limestone without compromising the material properties

[27]. For instance, Cetin et *al.*[28] state delayed dormant period and decreased total and rate of hydration heat when slag was blended with PLC. Moreover, the influences of slag on hydration and mechanical properties have been well conducted previously [29]. Lea[30] states hydration products of slag cement as tobermorite, ettringite, C_3A and portlandite; Scrivener and Nonat [31] report that alumina slows down C-S-H growth in the dormant stage of hydration; Dudovoy et *al.*[32] reveals the role of slag to perform compressive strength in blended cements; Roy and Idorn [33] found reduced heat rate in slag based combinations.

Besides, the positive effects of silica fume on cement-based materials is known [34] by reducing porosity [35] and improving the aggregate/paste transition zone. Also, it accelerates C_3S and C_3A hydration [34,36]. Indeed, a general consensus exists on the influence of SF on shortening the dormant period and the second major peak timing [37], and reducing the total hydration heat [38]. Kadri et *al.* state enhanced hydration at early age of LP/SF combination due to LP and at later ages due to the delayed pozzolanic activity of SF [39] ; Others report enhanced mechanical properties of Portland cement-limestone-silica fume combinations[40]. Besides, Turkel and Altuntas [41], by investigating self-consolidating repair mortars, confirm elevated mechanical properties of 5-10 % limestone powder combined with 20 % silica fume; and similar finding by Guneiyisi et *al.*, working on LP/slag/pozzolan self-consolidating concrete sets [42].

Thus, it seems that composite PLC/mineral admixture combinations may lead to improved hydration and engineering properties. Therefore, the main objective of this study is to investigate the influence of PLC/SF and PLC/LP combinations on hydration, compressive strength, sorptivity and microstructure of different types of mortar (having equivalent W/C ratio), where variables were mineral admixture’s (SF or LP) type and mortar's type (OMs, SCMs). This by characterizing hydration heat by semi-adiabatic calorimeter, Portlandite and

carboaluminate amounts through Thermogravimetric analysis, compressive strength, SEM imaging and water sorptivity.

For now, there are few investigations in the literature on the influence of slag blended PLC combined with chemical and mineral admixtures, especially in the cases of self-consolidating concretes/mortars. The authors suggest that hydration of such complex combinations is influenced by the chemical influence of superplastisizer and the physical packing of mortars (related to mortar type). Furthermore, relating hydration with macroscopic properties of the studied mortars should lead to better knowledge of the cementitious combinations, and provide some contributions on practical applications of composite PLCs.

In short, PLC/SF or PLC/LP combinations may have a performing effect on hydration and physic-chemical properties of the studied mixes.

2 Research Significance

LP-based cements and concretes provide a sustainable option to cut carbon emission. Ongoing research reveals the key features to get performed mixtures: finest particle size and appropriate limestone rate. Now we are aware that more mineral admixtures allow theorically increasing LP rate and greener material. However, blinded cements are very special materials, and are not available at any time in cement plants. The specifier hence may recommend more mineral admixtures (MAs) thought concreting to have the aimed engineering properties. Works on MAs added PLC-blended self-consolidating mixtures are scarce in the technical and scientific literatures. The authors believe this study may contribute to more knowledge to understand the mechanism and properties of blended-PLC/pozzolans sets and will be very useful to concrete technology.

3 Methodological Investigation

3.1 Chemical reactions and cementing materials in phase diagram

In this section, an attempt was made to simplify the chemical process involved in our cementitious combinations. That is, we present here the basilar reactions and establishing ternary diagram encompassing the studied cementing combinations.

According to Brunauer and Copeland[43] and Lea[30], the reactions formulas of the main phases leading to hydrates formation are written as follow[1]:

$$\underset{\text{(TricalciumSilicate)}}{2(C_3S)} + \underset{\text{(Water)}}{6Ħ} = \underset{\text{(Tobermorite)}}{C_3.S_2.Ħ_3} + \underset{\text{(Portlandite)}}{3Ca(OH)_2} \quad (1)$$

$$\underset{\text{(DicalciumSilicate)}}{2(C_2S)} + \underset{\text{(Water)}}{4Ħ} = \underset{\text{(Tobermorite)}}{C_3.S_2.Ħ_3} + \underset{\text{(Portlandite)}}{Ca(OH)_2} \quad (2)$$

$$\underset{\text{(TetracalciumAluminoferrite)}}{C_4AF} + \underset{\text{(Water)}}{10Ħ} = \underset{\text{(Portlandite)}}{2Ca(OH)_2} + \underset{\text{(Calcium Aluminoferrite Hydrate)}}{C_6.A.F.Ħ_{12}} \quad (3)$$

$$\underset{\text{(Tricalcium Aluminate)}}{C_3A} + \underset{\text{(Water)}}{12Ħ} + \underset{\text{(Portlandite)}}{Ca(OH)_2} = \underset{\text{(Tetracalcium Aluminate Hydrate)}}{C_3.A.Ca(OH)_2.Ħ_{12}} \quad (4)$$

$$\underset{\text{(Tricalcium Aluminate)}}{C_3A} + \underset{\text{(Water)}}{10Ħ} + \underset{\text{(Gypsum)}}{Ca.Š.Ħ_2} = \underset{\text{(Calcium Monosulfoaluminate)}}{C_3.A.CaŠ.Ħ_{12}} \quad (5)$$

After Gerry[44], in the presence of calcium sulfate, the product of hydration is a sulfoaluminate, $C_3A.3CŠ.H_{31–32}$, known as the mineral ettringite. It is a prismatic or acicular crystal shaped with a hexagonal cross-section.

$$\underset{\text{(Tricalcium Aluminate)}}{C_3A} + \underset{\text{(Water)}}{10Ħ} + \underset{\text{(Calcium Sulfate)}}{3C.Š.Ħ_2} = \underset{\text{(Ettringite)}}{C_3A.3CŠ.Ħ_{32}} \quad (6)$$

In this study, mortars include four cementitious combinations (related chemical phase calculations are given in Table 1). Thus, when placed in a ternary diagram (Figure 1), we can expect the nature of hydration products: With slag PLC (Cb2), more portlandite, AFm and some AFt; in combination Cb3, more portlandite and formation of AFt (ettringite) rather than AFm; on Cb4, formation of C-S-H with low S/C ratio, C-A-S-H compounds and silica gel.

[1] C= CaO, A=Al_2O_3, S=SiO_2, Ħ=H_2O, Š=SO_4

Furthermore, the presence of interground limestone is reported to form carboaluminate hydrate forms (As presented in the introduction).

3.2 Materials

For this test program, an ordinary Portland cement OPC (CEM I 52.5 N CE CP2 NF) was used in the reference mortar; interground slag PLC (CEM II/B-M(LL-S) 42.5 N CE CP) cement was used for the five other mortars. The cements meet the requirements of the EN 197-1 European standard[45] (equivalent to ASTM C105); a well graded 0/4 mm (# 8) fine aggregate was also used, with a silico-calcarous petrographic nature, meeting XP P18-545 standard requirements, and having a finesse modulus of 2.82. Furthermore, a Betocarb HP EB limestone powder, classed as '*A category'* according to NF P 18-508 standard, was implicated (average grain size da=20µm = 7.8 10^{-4} in.). Besides this, condensed silica fume (Condensil S95 DS) was also used. The main chemical and physical characteristics of the used cementing materials are presented in Table 2. A new generation of modified polycarboxylates superplasticizer has been used (Cimfluid Allegro 3010). Its main characteristics are presented in Table 3.

3.3 Mixture proportions, fabrication and curing

Three categories of mortars were considered in this investigation [Ordinary mortars (OMs), Self-consolidating mortars (SCMs), as their nomenclature is given in Table 4.We notice that the six mortars have been extracted from the mother concretes published previously by the authors[46], and adjusted then, to have appropriate fluidity for each type. The initial W/C ratio was 0.5, and the effective W/C was optimized as given in Table4. While O_{ref} mixture was based on OPC, O_{plc} was based on slag PLC. The ordinary mortars were mineral

admixture-free and served as references. $S_{plc}L$ and $S_{plc}S$ self-consolidating mortars were based on PLC and respectively on limestone powder and silica fume.

Ordinary mortars having a plastic consistency were fabricated and vibrated as per NF EN 196-1 standard[47], but additional four minutes waiting and one minute mixing at high speed were applied to avoid possible flash set[48,49] ; self-consolidating mortars were designed to have a target mortar spread of 240-260 mm (9,44-10,23 in.) after Sedran[50], and placed in molds without vibration.

For compressive strength, steel molds 40x40x160 mm (1.57x1.57x6.29 in.) were utilized. Furthermore, 40×40 mm (1.57×1.57 in.) cube molds were used for capillary absorption test. Samples were extruded from molds after one day and placed immediately underwater curing conditions until testing dates.

3.4 Test procedure

Specimens were brought out from water, and were air-dried in laboratory conditions for 24 hours. After that, compressive strength of mortars was determined by 3,7,28,56 and 91 days according to EN 196-1 standard [47].

Mortars' capillary absorption test was carried out in accordance to previous works[51]. Therefore, 40×40 mm (1.57×1.57 in.) cubes were adopted. First, mortar samples were cooled in room temperature for one week period to control their humidity rate. Then, they were oven-dried at 105 °C until a constant mass; placed on non-corrosive support in a 1 cm (0.39 in.) water pan filled. We note that the specimen's depth in contact with water was 5 mm (0.19 in.) (Figure 2). For a unidirectional flow, the samples' lateral area was covered with adhesive aluminum. Finally, by using a precision weighing balance the mass of specimens was

recorded to 0,5,10,20,30,60,180,360, and 1440 min, and the amount of the absorbed water was calculated. The capillary absorption coefficient (k) is obtained by the following formula:

$$\frac{Q}{A} = k\sqrt{t} \qquad (7)$$

Where Q = the amount of the adsorbed water in (cm^3); A= the cross section of the mortar sample in contact with water (cm^2); t= measuring timing (s); k= capillary absorption of the tested sample ($cm/s^{1/2}$). The coefficient (k) was graphically determined by plotting Q/A against $\sqrt{t}$, and calculated from the resulted slope of the.

Hydration heat test was conducted as per EN 196-9 standard [52], using the semi adiabatic calorimeter. This method consists of measuring the heat released during cement hydration using a thermally isolated Dewar flask. The test is carried out at 20C° monitored in air-conditioned room. Thus, temperature development during the period test (6 days) is defined as the difference between the temperatures of the tested mortar and inert mortar matured for a period superior than 3 moths. The mortar's temperature heat is the sum of the accumulated heat in the calorimeter, and the heat dispersed in the environment. At a time t, the hydration heat Q measured by gram of binder is obtained by applying the formula:

$$Q = \frac{C}{Mc}\Delta\theta + \frac{1}{Mc}\int_0^1 \alpha\Delta\theta dt \qquad (8)$$

Where C is the apparatus total thermal capacity (J/°C), Mc is the cement masse or binder mass (g), $\Delta\theta$ the difference in heating between mortar sample andthe ambientenvironment (°C), and α represents the total calorimeter thermal loss coefficient (J/h °C).

The rate of heat evolution is calculated using the following formula:

$$R_{heat} = \frac{(Qi-1 - Qi)}{(ti-1 - ti)} \qquad (9)$$

For thermal analysis, a 100 mg powder specimen was taken for each mortar and heated then in the thermal analyzer (STA 449 F1 Jupiter) with a 20°C/min rate. The objective of such test

is to quantify the hydration of cement mortars at medium and later ages. This by quantifying the portlandite (P) quantity developed through hydration, and measuring weight loss due to decarbonation served as indicator of the unreacted limestone amount. Surely data obtained by this test have a great significance to explain the physical properties of the tested mortars (compressive strength and water sorptivity).

Next, portlandite amount and decarbonation weight loss (in 3,28 and 91 days) were calculated according to Ref.[53].

$$\boldsymbol{p}(\%) = \frac{\boldsymbol{W550-W430}}{\boldsymbol{W1000}} \times \mathbf{100} \quad (10)$$

$$\boldsymbol{C}(\%) = \frac{\boldsymbol{W1000-W550}}{\boldsymbol{W1000}} \times \mathbf{100} \quad (11)$$

$$\boldsymbol{P}(\%) = \mathbf{4.11}.\boldsymbol{p} + \mathbf{1.68}.\boldsymbol{C} \quad (12)$$

With: p is the weight loss in TG curve at 430-550 °C, C is the weight loss at 550-1000 °C; P is the portlandite amount in the sample.

To assess the microstructural features, we used fractured specimens from mortars tested under the (JEOL 35CF) SEM. First, placed directly in an evaporator and maintained under high vacuum overnight. Then, gold-coated in evaporating apparatus just before getting the observations.

4 Experimental Results and Discussion

4.1 Compressive strength

Figure 3 shows the compressive strength results of mortar samples until 91 days hydration age.

On the influence of mortar type, it is obvious that SCMs exhibit equal to better compressive strength than OMs samples. This can be explained by the highest paste volume in SCMs and the beneficial dispersing effect of superplastisizer. We can observe too that 30 % of the

limestone powder in SplcL contributes better than 7 % silica fume in SplcS on compressive strength enhancement. It can be due to the good packing of the involved cementitious materials used in SplcL mortar. While the added limestone powder has better physical effect, interground limestone with clinker and slag in slag PLC cement has developed a chemical effect through the formed carboaluminate hydrate and the creation of additional nuclei sites.

By comparing OPC-based Oref and slag PLC-based Oplc, equivalent compressive strength can be seen at 3 and 14 days. However, at 7 and 91 days, PLC mortars exhibited 36 % better performance than OPC mortars. On one hand, the 7 days highest values of PLC mortar (27 MPa (3.91 Psi) compared to only 17 MPa (2.46 Psi) for OPC mortar) may be attributed to the chemical influence of inter-grounded LP (relatively accelerated hydration at early age as presented below in hydration heat section). One the other hand, the enhanced later compressive strength of Oplc can be due to the pozzolanic reaction provided by the inter-grounded slag.

For the optimal mixture SplcL, the authors believe that added and blended limestone powder may have a synergical effect when mixed with pozzolanic species. In that case a good compaction is guaranteed by physical packing and pronounced chemical reaction leading to more silica gel formation.

4.2 Water Sorptivity

Water sorptivity test results of all mortar specimens are given in Table 5. As expected, mortar sorptivity in this study follows a similar pattern of compressive strength values for all mortar types. Thereby, it is obvious that Oplc behaves better than Oref and SplcL mixtures was the best. The lower recorded sorptivity in SplcL mortar can be explained by the enhanced microstructure due to the cementitious combination of PLC and limestone powder [54], and the good adherence formed in the paste aggregate bond. Nevertheless, SplcS showed relatively higher sorptivity than Oref and SplcL. As discussed above, it seems that the

incorporated amount of silica fume in this combination (7%) was fewer than the optimum claimed in literature (10-15 %). By other words, a fewer quantity of SF cannot be totally dispersed in the mix leading to less involved materials in the pozzolanic reaction.

4.3 Early age hydration by Semi-Adiabetic Calorimetry

Figures 4 and 5 represent hydration heat development within 72 hours and the rate of heat release up to 28 hours, respectively. The first noticeable observation is the lowest heat and rate of hydration of PLC based combinations compared to the OPC reference mortar (40 % lower). What meant that the presence of mineral admixtures may lead to lesser heat release, and confirms that clinker amount in the binder is the main covering factor. Furthermore, for all mortar types, limestone-based combinations exhibited lower heat release than silica fume mixes. It can be explained the by the influence of the high SF pozzolanicity compared to the low reactivity of LP [37,55]. It is evident that heat and rate of hydration in the studied mortars can be classified as: OMs > SCMs. Again, this confirms that the amount of involved clinker and binder quantity are the most significant parameters regarding the heat of hydration.

Besides, in Figure 5, by comparing the rate of heat release in the second major peak, it can be seen that Oplc has 43 % lower values than Oref sample. In contrast, the acceleration stage in Oplc mortar starts at only one hour versus 2 hours recorded in Oref mortar. This makes a support to the existing findings by other researchers on the influence of carbonate additions on accelerating the rate of hydration at early ages [56,57]. However, in our case when slag PLC was used, the timing of the end of acceleration stage is not shortened compared to OPC mortar, as reported previously [58,59]. We recorded equivalent values for both Oref and Oplc mortar (11h). This fact may be attributed to the influence of slag combined with limestone in PLC fabrication, which by his retarding effect on hydration caused by its glassy structure[33], may neutralize limestone accelerating effect.

For SCMs mortar samples, delayed dormant period (5h for SplcL and 6h for SplcS) and 2nd peak timing (12h for SplcL and 13h for SplcS) were registered. Those results controvert some literature findings agreeing the accelerated hydration with limestone or silica fume[48], and meet some scholars' results[60]. In fact, the recorded delayed dormant period and the 2ndpeak timing can be explained by the cementitious combinations including clinker, slag, limestone or silica fume; and to the use of superplasticizer.

By relating compressive strength and rate of heat release results, one can conclude that enhancing compressive strength can be related to the longer delayed acceleration period. This conclusion makes sense when considering the nature of hydration products formed at this stage. Indeed, during that period the growth of S-C-H needles and silicate bearing products is accelerated [61,62].

4.4 Thermogravimetric analysis TGA

Portlandite and decarbonation loss by TG analysis for mortar samples up to 91 days is given in Table 6. With the presence of limestone powder, the test recorded high masse decarbonation loss and portlandite amount for SplcL, RplcL, and Oplc. This fact is well known[19], and explained by the presence of CaO as discussed in our ternary diagram.

In SF added mortars (SplcS), the portlandite hydrateseems to be consummated in later ages (28 or 91 days) due to the pozzolanic reaction monitored by silica fume and inter-ground slag. It is important to note that the co-existence of slag and silica fume leads to inconsistent portlandite consumption, as explained by some authors by the competition among mineral admixtures in the exhaustion of the existing portlandite [63].

Figure6 presents the derivative thermogravimetric curves (DTG) of all mortar samples at 3 days of hydration. Doing this task, we focused on carboaluminate characterization, detected approximately at 180°C in the DTG curve after some minutes. As found in previous works [64], carboaluminate peak in Oplc specimen was observed, but in SplcL mix a small peak

was formed. The authors explain this by the unreacted added limestone due to its coarser particle size. Thus, in this case we believe limestone powder has a physical rather than chemical effect.

4.5 SEM observations

Figure 7 (1-4) shows SEM observations of the mortars' fractured specimens (Oref, Oplc, SplcL and SplcS) at 28 days.

First, for Oref sample, the presence of ettringite needles 5μm ($1.9\ 10^{-4}$ in.) was observed. In fact, a poor crystallized reticular network of C-S-H was dominant[65] and occupy the majority of the paste. The presence of some unreacted clinker particles can be seen too. Due to its coarser size (> 10 μm =$3.9\ 10^{-4}$ in.), the portlandite hydrate may be partially hidden by smaller particles of inner C-S-H or ettringite. We note that the unreacted phases exist in all stages of hydration and may remain in this state with the narrowness of allowed space[66]. However, when morphological SEM observations are carried out, those unreacted materials are generally covered by C-S-H, ettringite or portlandite.

Second, for Oplc mortar, as expected and detected by TG results, the presence of portlandite due to carbonate excess in the mix was well observed. Besides, more refined C-S-H was observed in the monograph, which supports literature findings approving the growth hypothesis in the presence of carbonate[7]. Furthermore, smaller amounts of ettringite needles were remarked. This can be explained by the preferential formation of carboaluminate hydrate within the deceleration stage of hydration versus ettringite formation[67].

Third, for SplcL sample, the presence of plate-shaped portlandite and refined C-S-H hydrate was observed in the monograph. However, no ettringite was detected, may be to its conversion at this age (28 days) to monosulfate or monocarbonate hydrate. Besides, we can

see the denser microstructure that explain mechanical and water sorptivity achieved performance of this mortar.

Finally, for SpcS mortar sample, as detected by TG curves portlandite plates were observed in the specimen. What means that SF pozzolanic reaction at this stage doesn't consume the totality of portlandite. We interpreted in compressive strength and hydration degree section the lowest performance in this combination (PLC+ 7 % SF) by the insufficient amount of silica fume on the mix (Which doesn't lead to more announced pozzolanic reaction. Furthermore, the presence of C-S-H covering unreacted clinker was observed. It is assumed in previous works that with the presence of SF a low form of C-S-H is formed (having a C/S ratio about 0.8) [31], and lower portlandite forms nearing the interfacial area [68]. Well crystallized ettringite needles were also detected making like-bridges between cement grains.

5 Summary and concluding remarks

In this study some physical, hydration and microstructural investigations were carried out on two types of mortars. Based on the results of the investigation, the following conclusions are drawn.

Slag/limestone combination in PLC composite leads to enhanced properties of mortars both at early and later stages.

1. Self-consolidating mortars exhibited 36 % better compressive strength than OPC mortar, but lesser heat release and hydration degree. This meant that the mortar physical structure influences strongly the hydration and the resulted macro-properties.
2. The included limestone in slag PLC leads to good mechanical properties especially in SCMs mixes due to the dispersing effect of the superplastisizer. However, when

added to mortar it has a little contribution to enhance neither heat release nor hydration degree.

3. Combining blended and inter-ground limestone in the cementitious system should improve its packing (blended PLC), formation of more carboaluminate phase (interground PLC) and creating more nucleation site as template for S-C-H growth.

4. In SCMs mixes, the inter-ground limestone and slag present in the mix compete to react with the 7 % of silica fume. In this case, a higher amount of silica fume is needed to obtain higher reactivity and more mixture adhesion.

5. The amounts of clinker and superplasrisizer are significant parameters influencing the hydration mechanism. Increasing clinker leads to increased heat release and hydration degree but does not enhance the compressive strength. Adding more superplastisizer has beneficial effect on rheological properties and compressive strength, but extended dormant period should be occurred.

The study findings state the beneficial influence of limestone/pozzolanic admixtures combination, in production and use stages, to obtain more enhanced engineering properties of cementitious materials. The added limestone powder with PLC and/or silica fume hade a good synergical effect and led to better performance. Hence, the studied mixtures are greener, stronger and cheaper.

It is suggested therefore to carry out in-depth investigations on the influence of added limestone to composite PLCs, assessing other amounts of SF substitution and measuring the reactivity of the combined cementitious materials.

Compliance with Ethical Standards

Conflict of interest

The authors have no conflicts of interest to declare. All co-authors have seen and agree with the contents of this manuscript and there is no financial interest. We certify that the submission is original and is not under review at any other publication.

Ethical approval

This article does not contain any studies with human participants or animals performed by any of the authors.

REFERENCES

[1] Z. You-tang, Materials substitute evaluation in the production of cement, J. Wuhan Univ. Technol.-Mater Sci Ed. 17 (2002) 97–98.
[2] P.K. Mehta, Role of pozzolanic and cementious material in sustainable development of the concrete industry, ACI Spec. Publ. 178–1 (1998) 1–20.
[3] D.K. Panesar, R. Zhang, Performance comparison of cement replacing materials in concrete: Limestone fillers and supplementary cementing materials – A review, Constr. Build. Mater. 251 (2020) 118866.
[4] P.C.A., PCA outlines environmental, performance case for portland-limestone cement, (2020).
[5] Z. Zhang, Study on the structural build-up of cement-ground limestone pastes and its micro-mechanism, Constr. Build. Mater. 263 (2020) 120656.
[6] R. Sharma, S. Pandey, Influence of mineral additives on the hydration characteristics of ordinary Portland cement, Cem. Concr. Res. 29 (1999) 1525–1529.
[7] E. Berodier, K. Scrivener, Understanding the Filler Effect on the Nucleation and Growth of C-S-H, J. Am. Ceram. Soc. 97 (2014) 3764–3773.
[8] K. Ingram, Carboaluminate reactions as influenced by limestone additions. Carbonate additions to cement, ASTM STP 1064, in: R.D. P.Klieger, Hooton (Eds.), Phila. Am. Soc. Test. Mater., 1990: pp. 14–23.
[9] B. Lothenbach, Influence of limestone on the hydration of Portland cements, Cem. Concr. Res. 38 (2008) 848–860.
[10] G. Kakali, Hydration products of C 3 A, C 3 S and Portland cement in the presence of CaCO 3, Cem. Concr. Res. 30 (2000) 1073–1077.
[11] G.D. Moon, Effects of the fineness of limestone powder and cement on the hydration and strength development of PLC concrete, Constr. Build. Mater. 135 (2017) 129–136.
[12] A.-M. Poppe, G. Schutter, Cement hydration in the presence of high filler contents, Cem. Concr. Res. 35 (2005) 2290–2299.

[13] P. Kathirvel, Strength and durability properties of quaternary cement concrete made with fly ash, rice husk ash and limestone powder, Arab. J. Sci. Eng. 38 (2013) 589–598.
[14] S. Liu, P. Yan, Effect of limestone powder on microstructure of concrete, J. Wuhan Univ. Technol.-Mater Sci Ed. 25 (2010) 328–331.
[15] G.K. Moir, S. Kelham, Developments in the manufacture and use of Portland limestone cement, ACI Spec. Publ. 172 (1999) 797–820.
[16] V. Bonavetti, High-strength concrete with limestone filler cements, ACI Spec. Publ. 186 (1999) 567–580.
[17] J. Péra, Influence of finely ground limestone on cement hydration, Cem. Concr. Compos. 21 (1999) 99–105.
[18] Y. Zhao, Y. Zhang, A Review on Hydration Process and Setting Time of Limestone Calcined Clay Cement (LC3), Solids. 4 (2023) 24–38.
[19] R. Hooton, Portland-limestone cement: state-of-the-art report and gap analysis for CSA A 3000, Cement Association of Canada. University of Toronto, 2007.
[20] B.S. Hansen, Portland-Limestone Cement Fineness Effects on Concrete Properties, ACI Mater. J. 117 (2020) 157–168.
[21] H. Rong, Z. Zhou, S. Peng, Y. Huang, J. Liang, X. Yang, J. Shi, Y. Feng, Effect of ultra-fine limestone powder on leaching resistance of cement mortar, Constr. Build. Mater. 368 (2023) 130422.
[22] A. Marzouki, A. Lecomte, Durability of Cementitious Composites Mixed with Various Portland Limestone Cement-Cements, ACI Mater. J. 114 (2017) 763.
[23] A.A. Ramezanianpour, Influence of various amounts of limestone powder on performance of Portland limestone cement concretes, Cem. Concr. Compos. 31 (2009) 715–720.
[24] E.F. Irassar, Mechanical properties and durability of concrete made with portland limestone cement, ACI Spec. Publ. 202–27 (2001) 431–450.
[25] A. Soltani, A. Tarighat, M. Varmazyari, Calcined marl and condensed silica fume as partial replacement for ordinary portland cement, Int. J. Civ. Eng. 16 (2018) 1549–1559.
[26] O. Rudić, N. Ukrainczyk, M. Krüger, J. Tritthart, J. Juhart, Efficiency of limestone in clinker-reduced binders: Consideration of water-binder ratio, capillary porosity and compressive strength, Constr. Build. Mater. 386 (2023) 131594.
[27] A. Arora, Ternary blends containing slag and interground/blended limestone: Hydration, strength, and pore structure, Constr. Build. Mater. 102, Part 1 (2016) 113–124.
[28] C. Çetin, S.T. Erdoğan, M. Tokyay, Effect of particle size and slag content on the early hydration of interground blended cements, Cem. Concr. Compos. 67 (2016) 39–49.
[29] R.A. Hawileh, J.A. Abdalla, F. Fardmanesh, P. Shahsana, A. Khalili, Performance of reinforced concrete beams cast with different percentages of GGBS replacement to cement, Arch. Civ. Mech. Eng. 17 (2017) 511–519.
[30] F.M. Lea, The chemistry of cement and concrete, Edward Arnold Publishers Limited, London, 1970.
[31] K.L. Scrivener, A. Nonat, Hydration of cementitious materials, present and future, Cem. Concr. Res. 41 (2011) 651–665.
[32] V.S. Dubovoy, Effects of ground granulated blast-furnace slags on some properties of pastes, mortars, and concretes, ASTM Spec. Tech. publication(897 (1986) 29–48.
[33] D.M. Roy, G.M. ldorn, Hydration, Structure, and Properties of Blast Furnace Slag Cements, Mortars, and Concrete, ACI J. 79 (1982) 444–457.
[34] T.C. Holland, Guide for the use of silica fume in concrete, 2000.
[35] R. Hooton, Influence of silica fume replacement of cement on physical properties and resistance to sulfate attack, freezing and thawing, and alkali-silica reactivity, ACI Mater. J. 90 (1993) 143–151.

[36] S. Hoshino, XRD/Rietveld analysis of the hydration and strength development of slag and limestone blended cement, J. Adv. Concr. Technol. 4 (2006) 357–367.
[37] E.H. Kadri, R. Duval, Effect of ultrafine particles on heat of hydration of cement mortars, ACI Mater. J. 99 (2002) 138–142.
[38] I. Meland, Influence of condensed silica fume and fly ash on the heat evolution in cement pastes, ACI Spec. Publ. 79 (1983) 665–676.
[39] E. Kadri, Combined effect of chemical nature and fineness of mineral powders on Portland cement hydration, Mater. Struct. 43 (2010) 665–673.
[40] V. Bilek, Development and properties of concretes with ternary binders, Cem. Wapno Beton. 79 (2013) 343–352.
[41] S. Turkel, Y. Altuntas, The effect of limestone powder, fly ash and silica fume on the properties of self-compacting repair mortars, Sadhana. 34 (2009) 331–343.
[42] E. Güneyisi, M. Gesoğlu, Properties of self-compacting portland pozzolana and limestone blended cement concretes containing different replacement levels of slag, Mater. Struct. 44 (2011) 1399–1410.
[43] S. Brunauer, L. Copeland, The chemistry of concrete, Sci. Am. 210 (1964) 80–99.
[44] B. Gerry, Portland Cement, Thomas Telford, London, 2011.
[45] A.F.N.O.R., EN 197-1: Cement - Part 1: Composition, specifications and conformity criteria for common cements, (2000).
[46] T. Chiker, S. Aggoun, H. Houari, R. Siddique, Sodium sulfate and alternative combined sulfate/chloride action on ordinary and self-consolidating PLC-based concretes, Constr. Build. Mater. 106 (2016). https://doi.org/10.1016/j.conbuildmat.2015.12.123.
[47] A.F.N.O.R., EN 196-1: Méthodes d'essais des ciments–Partie 1: détermination des résistances mécaniques, AFNOR, 2006.
[48] M. Maage, Strength and heat development in concrete: Influence of fly ash and condensed silica fume, ACI Spec. Publ. 91 (1986) 923–940.
[49] A.M. Neville, Properties of Concrete, Trans-Atlantic Publications,Indian International Ed, 2011.
[50] T. Sedran, Rheologie et rheometrie des betons: Application aux betons autonivelants, Doctorate Thesis, Ecole Nationale des Ponts et Chaussées, 1999.
[51] T. Gonen, S. Yazicioglu, The influence of compaction pores on sorptivity and carbonation of concrete, Constr. Build. Mater. 21 (2007) 1040–1045.
[52] A.F.N.O.R., EN 196-9: Standard : Methods for testing cements, (2010).
[53] B. El-Jazairi, J. Illston, A simultaneous semi-isothermal method of thermogravimetry and derivative thermogravimetry, and its application to cement pastes, Cem. Concr. Res. 7 (1977) 247–257.
[54] W. Zhu, P. Bartos, Permeation properties of self-compacting concrete, Cem. Concr. Res. 33 (2003) 921–926.
[55] E.H. Kadri, R. Duval, Effect of Silica Fume on the Heat of Hydration of High-Performance Concrete, ACI Spec. Publ. 199 (2001) 635–644.
[56] R. Hooton, Effects of carbonate additions on heat of hydration and sulfate resistance of Portland cements. Carbonate additions to cement, 1064 ASTM STP, in: P. Klieger, R. Hooton (Eds.), Phila. Am. Soc. Test. Mater., 1990: pp. 73–81.
[57] V. Rahhal, Role of the filler on Portland cement hydration at early ages, Constr. Build. Mater. 27 (2012) 82–90.
[58] V. Rahhal, Calorimetric characterization of Portland limestone cement produced by intergrinding, J. Therm. Anal. Calorim. 109 (2012) 153–161.
[59] B. Yılmaz, A. Olgun, Studies on cement and mortar containing low-calcium fly ash, limestone, and dolomitic limestone, Cem. Concr. Compos. 30 (2008) 194–201. https://doi.org/10.1016/j.cemconcomp.2007.07.002.

[60] W. Nocuń-Wczelik, B. Trybalska, Effect of admixtures on the rate of hydration and microstructure of cement paste, Cem. Wapno Beton. 6 (2004) 284–289.
[61] D. Double, A. Hellawell, The solidification of cement, Sci. Am. 237 (1977) 82–91.
[62] A. Bazzoni, Study of early hydration mechanisms of cement by means of electron microscopy, EPFL, 2014.
[63] M. Baalbaki, S. Sarker, P. Aitcin, H. Isabelle, Properties and microstructure of high-performance concretes containing silica fume, slag and fly ash, Spec. Publ. 132 (1992) 921–942.
[64] K. Celik, R. Hay, C.W. Hargis, J. Moon, Effect of volcanic ash pozzolan or limestone replacement on hydration of Portland cement, Constr. Build. Mater. 197 (2019) 803–812.
[65] H.M. Jennings, A model for the microstructure of calcium silicate hydrate in cement paste, Cem. Concr. Res. 30 (2000) 101–116.
[66] P. Barnes, J. Bensted, Structure and performance of cements, CRC Press, 2002.
[67] N. Voglis, S. Tsvilis, G. Kakali, E. Chaniotakis, C. Meletiou, Limestone, fly ash, slag and natural pozzolana: a comparative study of their effect on the cement properties, in: Mod. Concr. Mater. Bind. Addit. Admix., Thomas Telford Publishing, 1999: pp. 203–210.
[68] L. Zhang, N. Ma, Y. Wang, B. Han, X. Cui, X. Yu, J. Ou, Study on the reinforcing mechanisms of nano silica to cement-based materials with theoretical calculation and experimental evidence, J. Compos. Mater. 50 (2016) 4135–4146.

Tables and Figures

List of Tables:

List of Figures:

TABLES

Table 1–Calculations of CaO, SiO_2, and AlO_3 contents for cementitious combinations (based on Figure 1).

	Cb1(%)	Cb2(%)	Cb3(%)	Cb4(%)
SiO_2	20.6	17.1	11.9	22.6
Al_2O_3	4.5	6.4	4.5	6
CaO	63.4	68.9	75.5	64.1

Table 2– Physical and chemical characteristics of cementing materials (by mass) – Data from the producer technical sheets.

Chemical characteristics (%)				
	OPC	*PLC clinker (75 %)*	*LP*	*SF*
$Si\ O_2$	20.6	21.54	-	95
$Fe\ O_3$	2.4	2.62	-	-
$Al_2\ O_3$	4.5	4.91	-	-
Ca O	63.4	66.77	96.3	1
Mg O	1.9	-		-
SO_3	3.2	2.9	0.003	2
$K_2\ O$	0.76	-	-	-
$Na_2\ O$	0.11	-	-	0.6
LI **	0.024	0.071	-	-
Cl^-	0.04	0.03	0.002	0.1
Physical characteristics				
SG***	3.16	3.1	2.7	2.24
Blaine (m^2/kg)	425	-	435	25000
* Mineralogical Composition (%) : OPC: C_3S=68;C_2S=10; C_3A=8; C_4AF=8 PLC : C_3S=66.7;C_2S=11.6; C_3A=8.6; C_4AF=8 ** Lost of Ignition *** Specific gravity				
PLC-included Limestone (17%) **PLC-included slag (8%)** CaCO3(%) = 90.8 (CaO+MgO)/SiO2 > 1 CaO+MgO+SiO2 > 66 Vitreous slag (%) > 66				

Table 3– The main Characteristics of the superplasticizer (from:http://fra.sika.com/fr/solutions-produits.html)

density	pH	Cl – (%)	Na_2 O Eq. (%)	Extract (%)
1,08	4,8	0,1	0,2	32

Notes: for density 1 kg/m^3= 6.24 10^{-2} lb/ft^3

Table 4 – 1m3 Mixture composition of mortars.

	Sand (kg)	Cement (kg)	S/C	LP (kg)	SF (kg)	Addition (%)	Water (kg)	Sup. (l)	W/Ceff	Beq=C+kA	W/Beq
$\mathbf{O_{ref}}$	1440	480	3				275		0.57	480	0.57
$\mathbf{O_{plc}}$	1440	480	3				260		0.54	480	0.54
$\mathbf{S_{plc}L}$	1302	442	2.95	208		32	235	9	0.53	494	0.48
$\mathbf{S_{plc}S}$	1448	453	3.20		34	6,98	240	9.5	0.53	487	0.49

*B_{EQ}= C+kA (A=Addition , k_{LF} = 0.25 , k_{SF}= 2 if W/C≤0.45 and C≥295 if not k_{SF}=1). See EN 206-1 Standard.

Notes: 1 kg= 2.204 lb. , 1 l = 0.264 US Gallon , 1m^3 = 35.31 ft^3

Table 5– Sorptivity Coefficients of mortar samples.

Mixture Code	Sorptivity Coefficient $\times 10^{-3}$. cm/$s^{0.5}$
Oref	1.76
Oplc	1.56
SplcL	1.42
SplcS	1.93

Table 6– Portlandite and decarbonation masse loses by TG analysis for mortar samples.

	3 days		28 days		91 days	
	P (%)	C (%)	P (%)	C (%)	P (%)	C (%)
Oref	16.70	6.98	15.78	5.85	18.32	7.36
Oplc	18.32	8.09	20.46	8.93	17.74	7.58
SplcL	22.07	11.08	21.70	10.96	22.97	11.08
SplcS	16.87	8.11	21.32	9	15.04	6.9

FIGURES

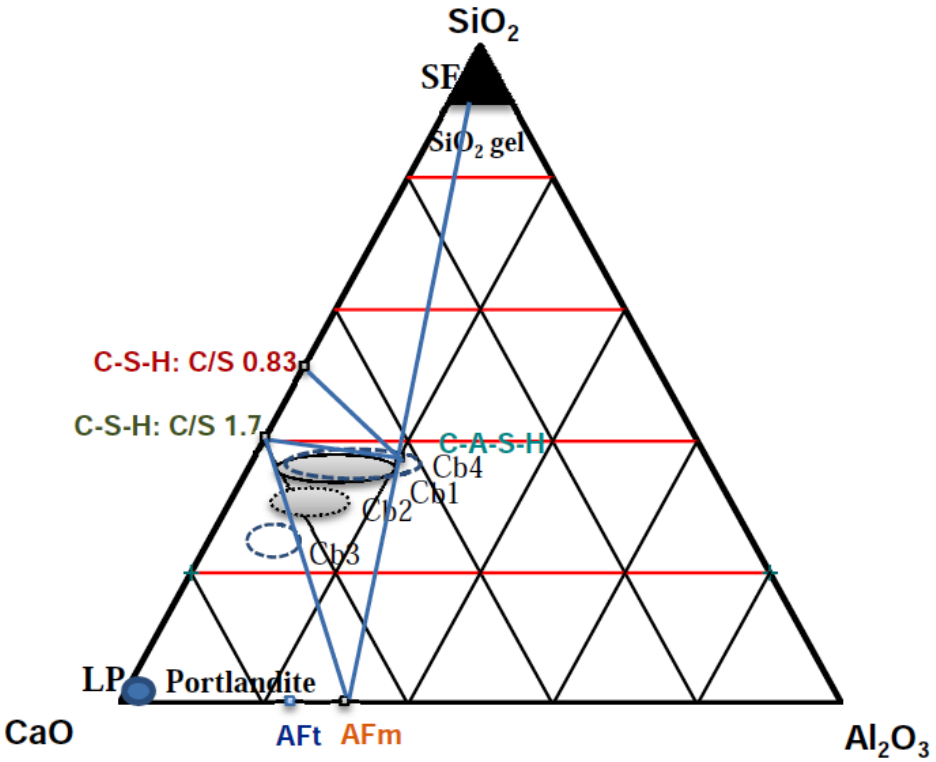

Figure 1– Ternary diagram CaO-SiO_2-AlO_3 for cementitious combinations.

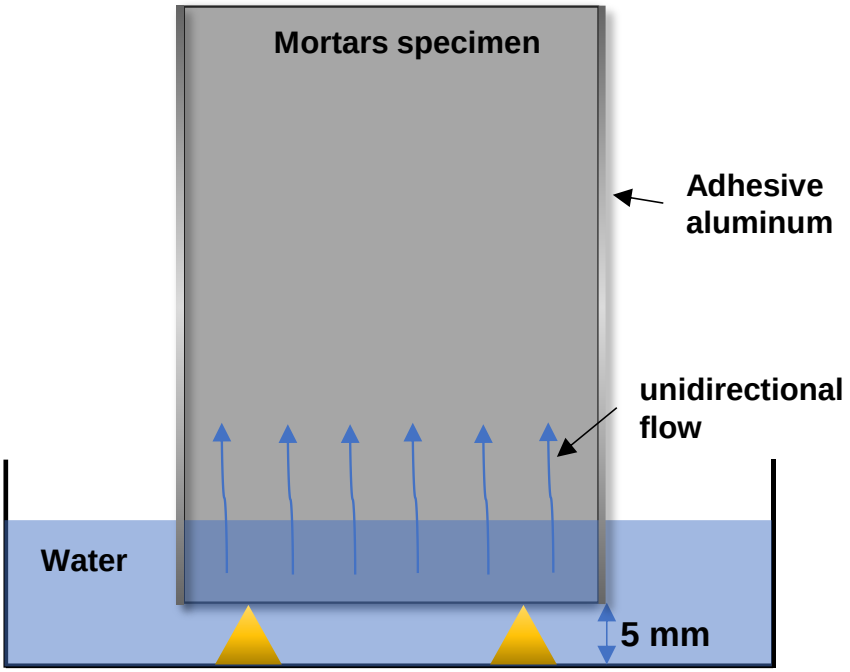

Figure 2 –Water sorptivity measurement of mortars' samples

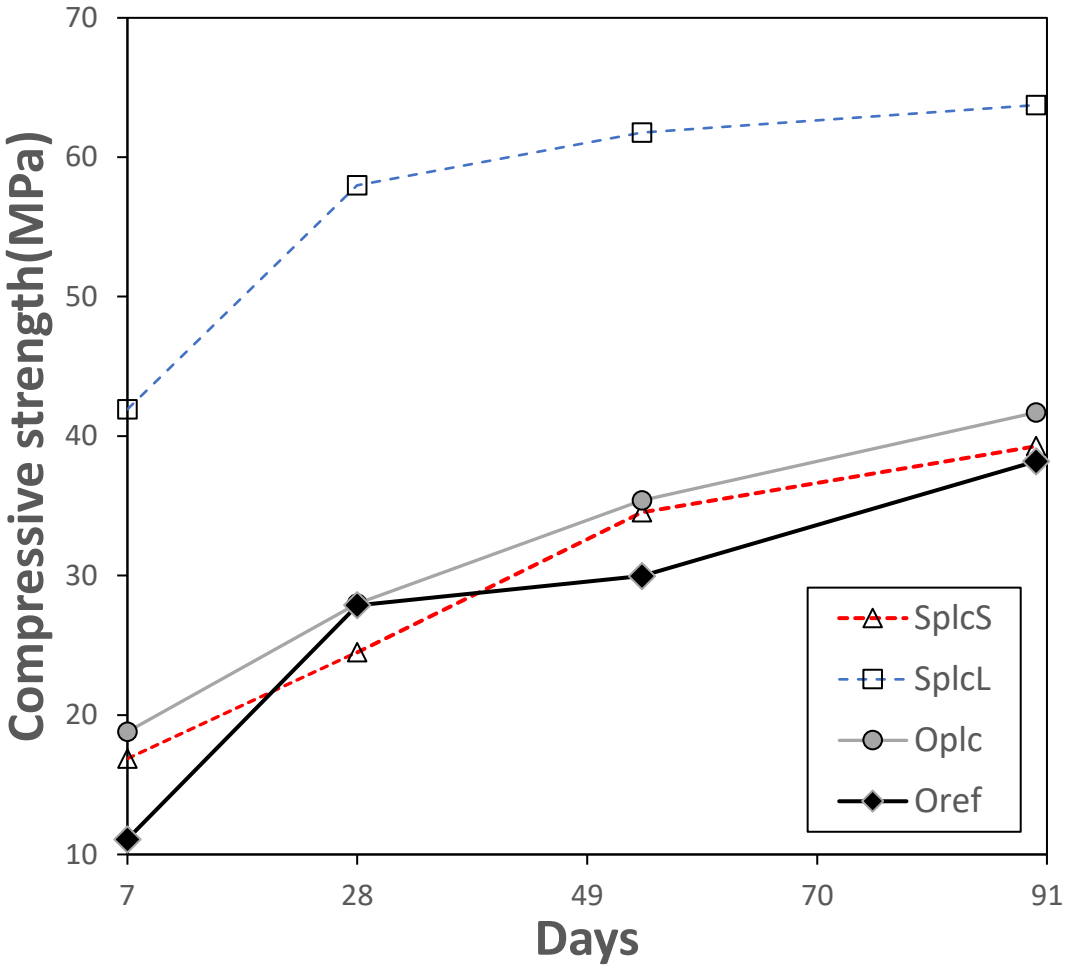

Figure 3–Compressive strength of mortar samples.

Notes: 1MPa= 145,038 Psi

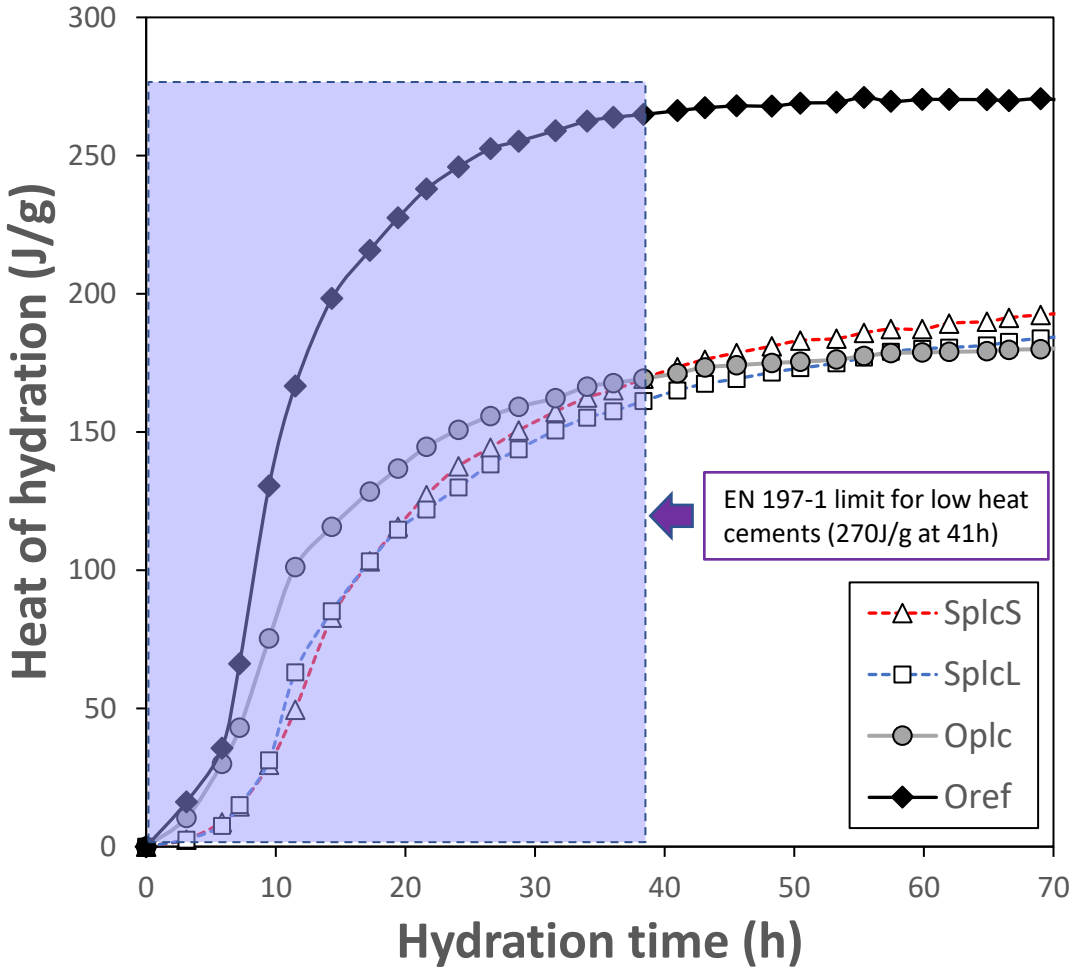

Figure 4– Hydration heat development of mortar samples in the Semi-Adiabetic Calorimeter within 72 hours (NF EN 196-9).

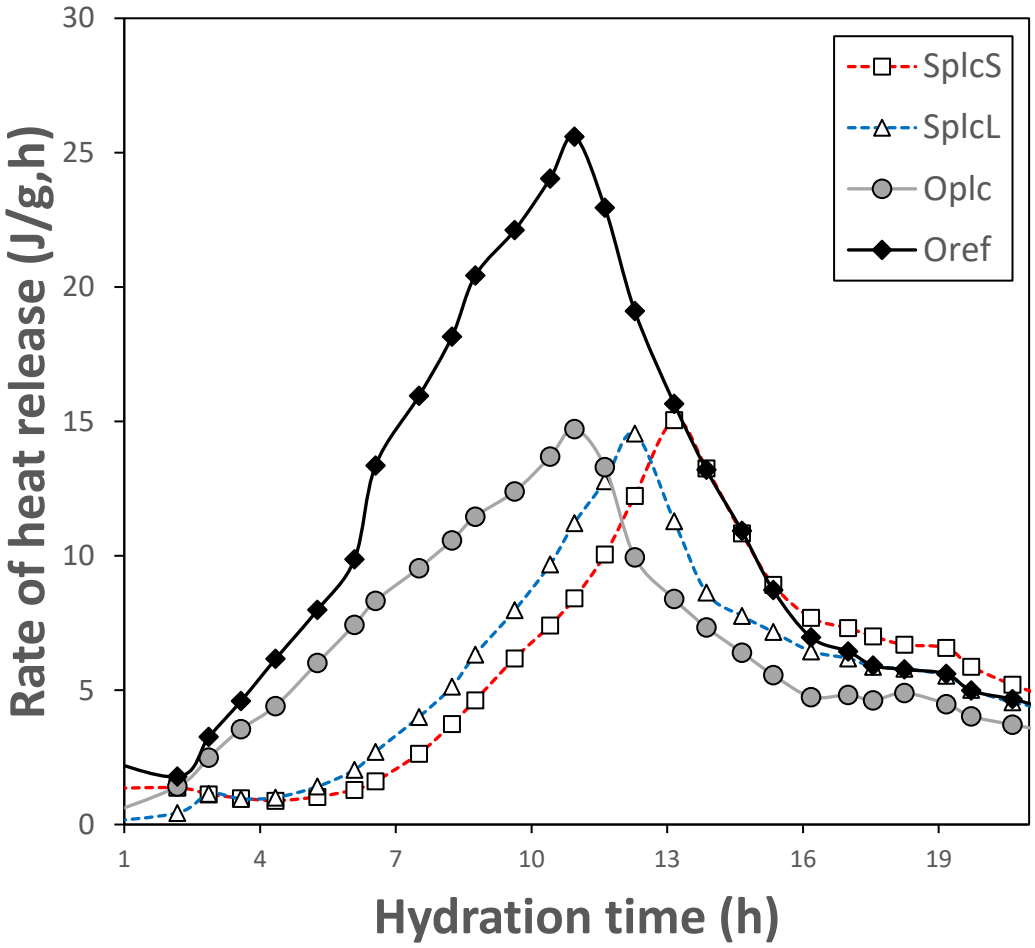

Figure 5– Rate of heat release versus hydration time for mortar samples.

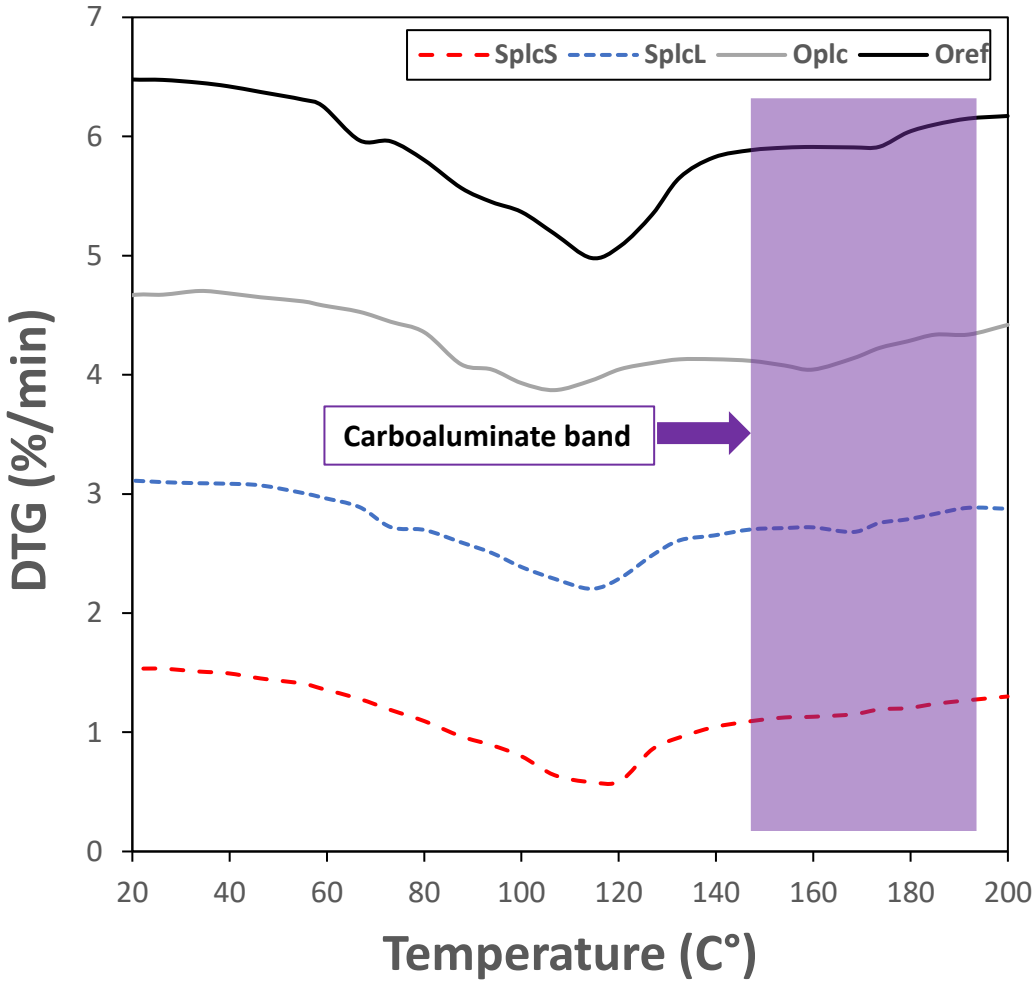

Figure 6– Carboaluminate characterization by DTG curves.

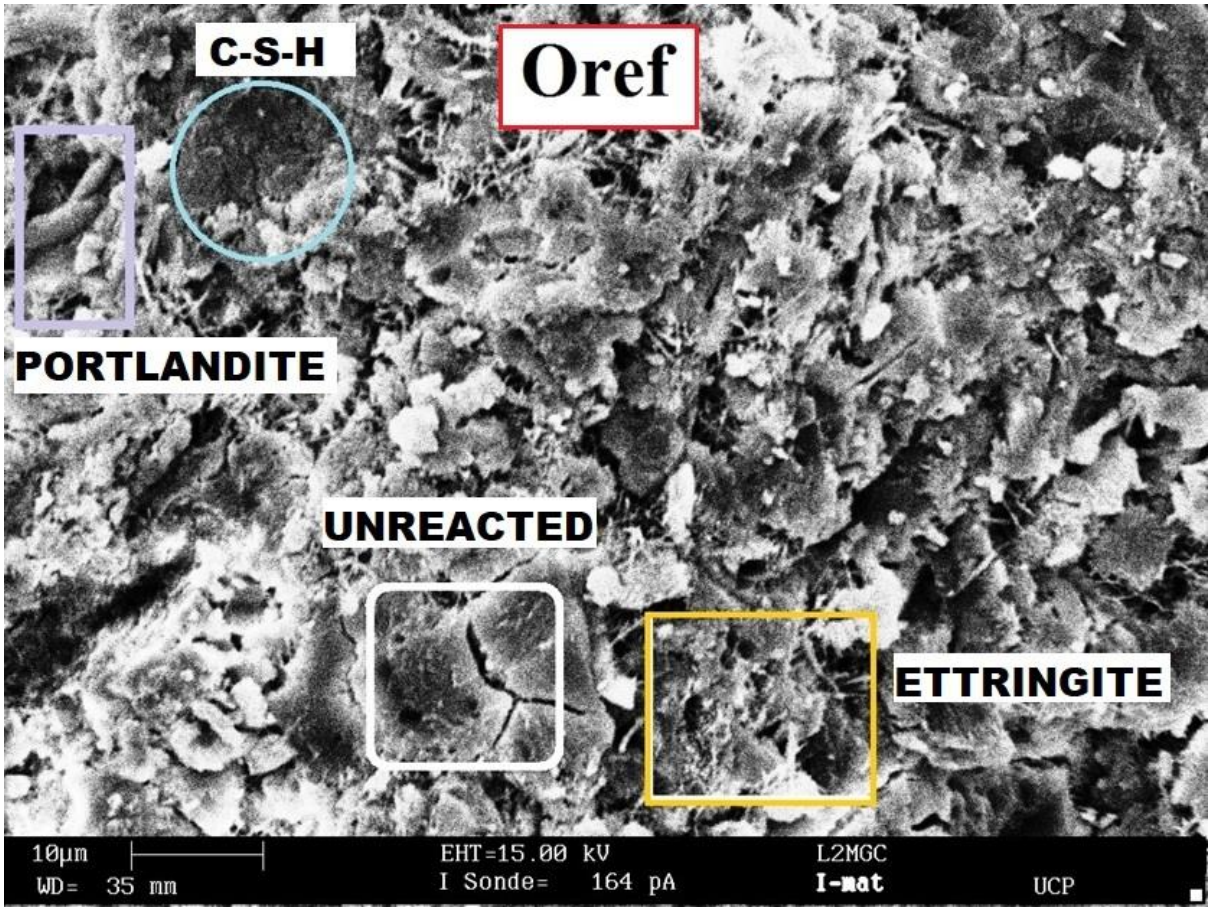

Figure 7.1 – SEM images of mortar fracture specimens of Oref.

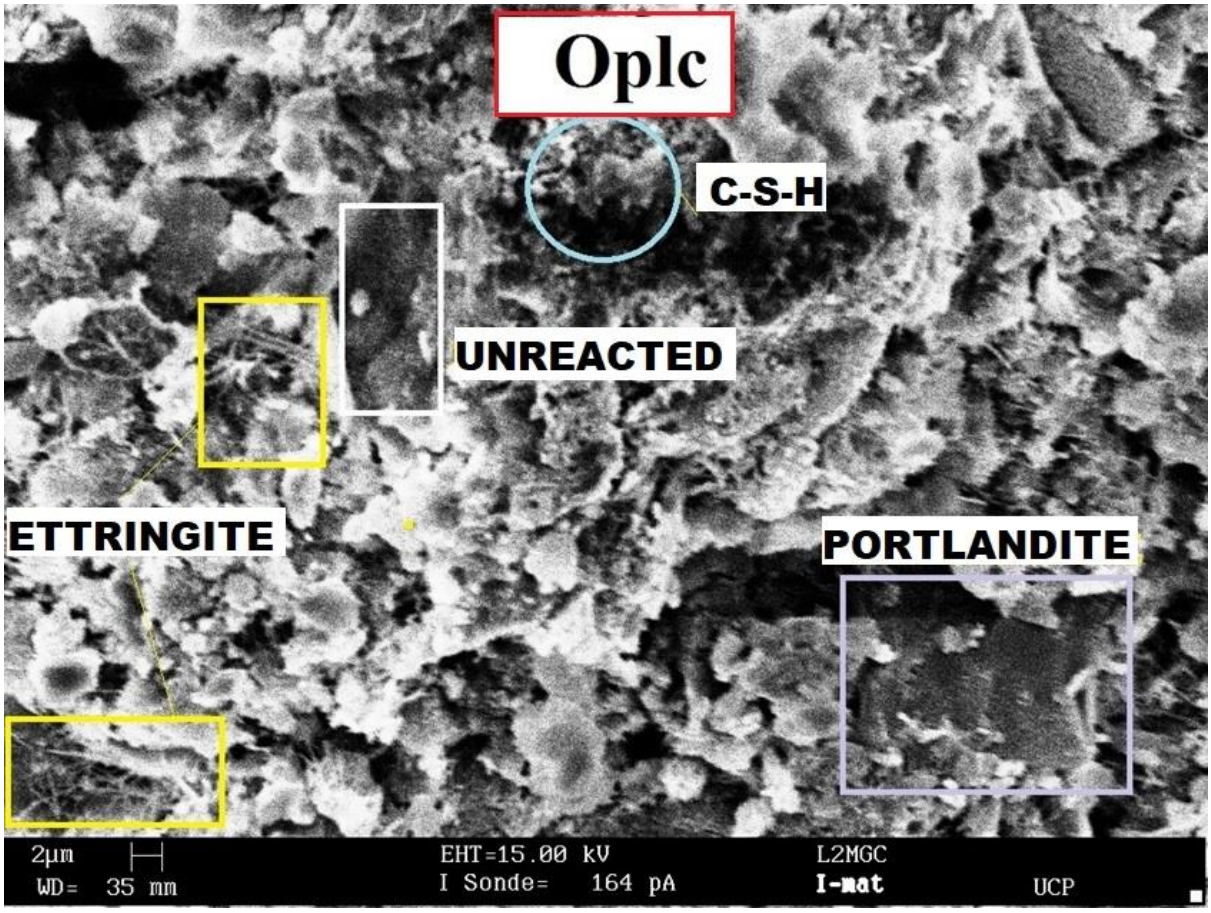

Figure 7.2 – SEM images of mortar fracture specimens of Oplc.

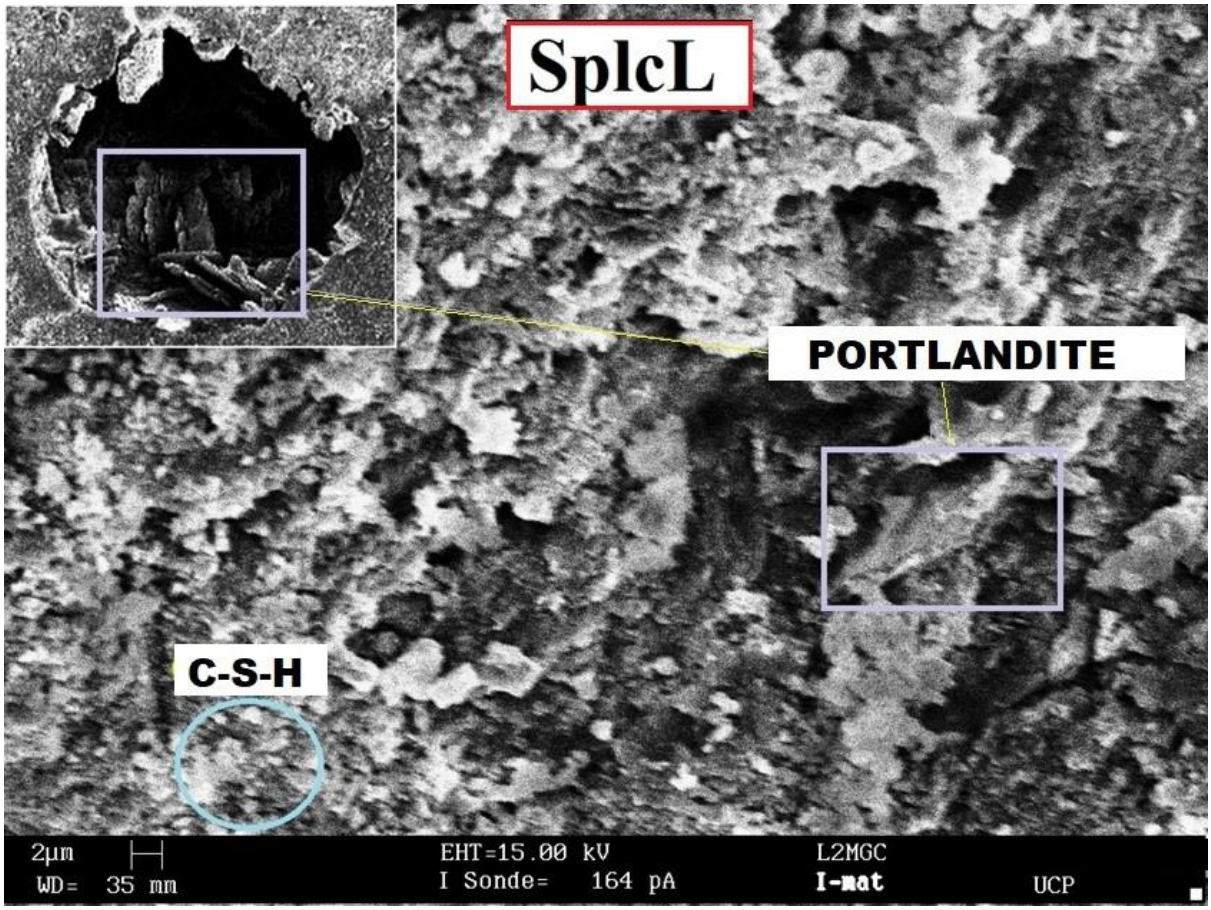

Figure 7.3 – SEM images of mortar fracture specimens of SplcL.

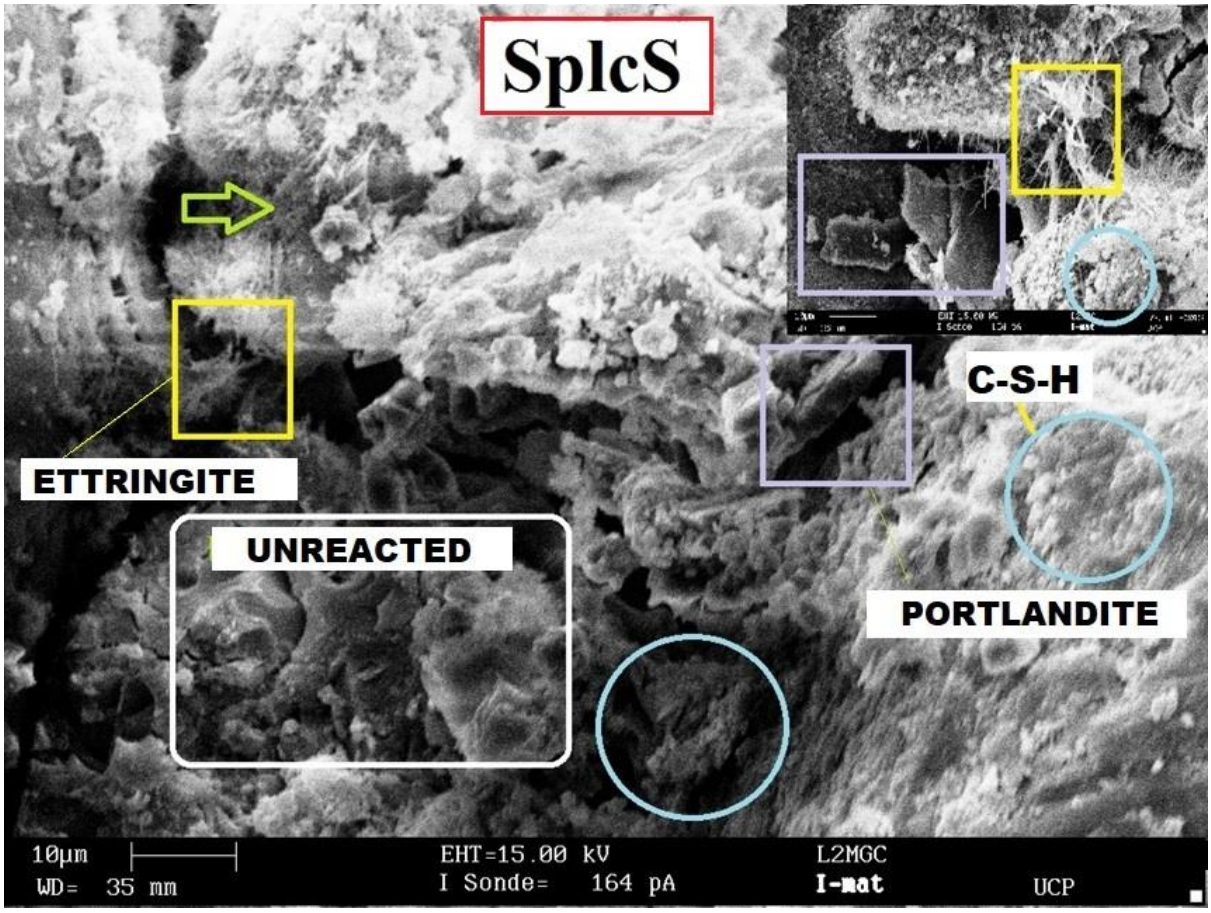

Figure 7.4 – SEM images of mortar fracture specimens of SplcS .